Prediction Study of Structural, Elastic, Electronic, Optical and Thermodynamic Properties of Cubic Perovskite Bigao3

M. A. Ghebouli
University Ferhat Abbas of Setif
B. Ghebouli
University Ferhat Abbas of Setif
M. Fatmi (fatmimessaoud@yahoo.fr)
University Ferhat Abbas of Setif
T. Chihi
University Ferhat Abbas of Setif
S. I. Ahmed
Taif University

Research Article

Keywords: cubic perovskite BiGaO3, optical properties, first principle

Posted Date: March 12th, 2021

DOI: https://doi.org/10.21203/rs.3.rs-275574/v1

Prediction Study of structural, elastic, electronic, optical and thermodynamic properties of cubic perovskite $BiGaO_3$

M.A. Ghebouli [1, 2], B. Ghebouli [3], M. Fatmi [2,*], T. Chihi [2], S. I. Ahmed [4]

[1] *Department of Chemistry, Faculty of Technology, University of Mohamed Boudiaf, M'sila, 28000, Algeria.*
[2] *Research Unit on Emerging Materials (RUEM), University of Setif 1, 19000, Algeria.*
[3] *Laboratory of Studies Surfaces and Interfaces of Solids Materials, Department of Physics, Faculty of Science, University Ferhat Abbas of Setif 1, Setif 19000, Algeria.*
[4] *Department of Physics, College of Science, Taif University, P.O. Box 11099, Taif 21944, Saudi Arabia.*

***Corresponding author :** fatmimessaoud@yahoo.fr

Abstract

We report computations of all properties cited in title within GGA and LDA for cubic perovskite $BiGaO_3$. Lattice constants, bulk modulus, elastic moduli and band gaps were computed. BiGaO3 is elastically stable at room temperature and equilibrium pressure. We predicted the Debye temperature and longitudinal and transverse waves along [100], [110] ([100], [110], [111]) directions for $BiGaO_3$. Our calculated band gap 1.92 eV predicts the semiconducting nature. The upper valence band is consisted principally of O-2p sites and a little contribution of Ga-4p and Bi-6p states. Hybridization between Ga-4p orbital with O-2p site in the upper valence band traduces that Ga–O bonds have a covalent bonding character. B/G ratio indicates that $BiGaO_3$ is classified as ductile material. We derived mechanical parameters of $BiGaO_3$ using Voigt, Reuss and Hill approximations. The higher absorption value provides a hint that this material is a potential candidate as a photo catalyst in the degradation of chemicals or pollutants.

Keys words: cubic perovskite $BiGaO_3$ **;** optical properties ; first principle

1. Introduction

Perovskite oxides have attracted particular interest for their applications in the ferroelectric and piezoelectric fields and also as multiferroids [1-3]. The materials used in ferroelectric and piezoelectric devices are lead-based compound which are toxic. Therefore, it is necessary to look for a new material as a replacement and that shows the same characteristics but less harmful for the environment. The search and development for such an alternative piezoelectric materials is now a

very active research topic and leads on bismuth-layer structure. Bismuth layer structure posses a high Curie temperature, high mechanical quality factor, large dielectric breakdown strength, good aging characteristics, and have good piezoelectric properties, which make them candidate materials for ceramic filter and resonator applications. Bi-based compounds are the most candidat as individual lead-free piezoelectrics because they are nontoxic and have $6s^2$ lone pairs, which is the origin of large ferroelectric polarizations [4, 5]. The pérovskite oxydes bismuth gallate $BiGaO_3$ (Ga is nonmagnetic ion) crystallized in the cubique, hexagonal, tétragonal and orthorhombic structures. Experiment results show that at the ambient pressure, $BiGaO_3$ crystallizes in the orthorhombic structure. Although a number of theoretical studies exploring structural, elastic and electronic properties of $BiGaO_3$ compound have been carried out for the ideal cubic [6, 7] and orthorhombic modifications [8-10] of the perovskite structure. Bismuth gallate $BiGaO_3$ was experimentally synthesized using a high pressure and at high temperature technique [11]. The experiment investigations [12-14] for exploring the physical properties of bulk and nanostructures of these compounds are limited as compared to other multi-ferroic materials.

In this work, we focus on the detailed study of structural, elastic, electronic, optical and thermodynamic properties of cubic bismuth gallate $BiGaO_3$ within GGA and LDA using the plane waves pseudo-potentiel method of density functionel theory (DFT). The theoretical model of this paper is firstly explained. After that, the computed results are analyzed in the second part. In the end, we conclude the present work.

2. Computational method

Computations are carried out by (CASTEP) code [15]. Kohn–Sham equations are treated by DFT frame-work [16, 17], where wave functions of valence electrons have smaller kinetic energy cut-off energy. Vanderbilt-type ultra soft pseudo-potential [18] in reciprocal space is used to represent the interaction of valence electrons with ion cores. GGA of Perdew et al. [19] and LDA of Teter and Pade parameterization [20] are adopted for the exchange-correction functional. The discret summation over k-points scheme of Monkhorst– Pack [21] replaces integrations in the Brillouin zone. Cut-off energy of 660 eV and k-points 8×8×8 are used to ensure well convergence of structures and energies. Optical parameters computation requires the use of uniformly distributed k-points 20×20×20. Structural parameters were determined by BFGS minimization technique [22]. The tolerance for geometry optimization was total energy 5×10^{-6} eV/atom, maximum ionic Hellmann-Feynman force 10^{-2} eV/Å and maximum stress $2\text{x}10^{-2}$ eV/Å^3. The quasi-harmonic Debye model is used in thermal effect to describe the variation E(V) [23]. Gibbs program evaluates Debye

temperature, obtains G (P, V, T) and minimize it and derives V (P, T). Detailed description of this model can be found in [24-27].

3. Results and discussion

3. 1. Ground state properties

Perovskite oxide $BiGaO_3$ is modeled in ideal cubic structure. The cubic unit cell is consisting of unit formula with Wyckoff positions of the atoms Bi:1a (0, 0, 0), Ga:1b (1/2, 1/2, 1/2) and O:3c (1/2, 1/2, 0). The electronic configurations of Bi, Ga and O atoms are Bi: [Xe] $4f^{14}$ $5d^{10}$ $6s^2$ $6p^3$, Ga: [Ar] $3d^{10}$ $4s^2$ $4p^1$ and O: $1s^2$ $2s^2$ $2p^4$. The pressure behavior of $BiGaO_3$ structural parameters requires, that geometry of cell at equilibrium is calculated at pressure ranging from 0 to 40 GPa. The complete optimization of structural parameters is performed at each pressure. The pressure as a function of normalized volume is visualized in Fig. 1 with respect to fit Murnaghan [28]. The computed lattice parameters as extracted from this geometry are listed in Table 1. Our structural parameters performed by GGA are closer to previous calculations carried out within the Wien2k computer code [29]. One can notice that the LDA value of lattice constant (bulk modulus) is lower (greater) than that given by GGA. In a cubic structure, the bulk modulus is a good indicator of hardness because it is linked to isotropic deformation [30]. The results show that $BiGaO_3$ has high bulk modulus, which is a sign of strong hardness.

3. 2. Elastic constants

The cubic system is characterized by three different symmetry elements (C_{11}, C_{12}, and C_{44}), estimated by determining the stress tensor under strain application to the optimized structure. Elastic constants give information on binding between adjacent atoms, the anisotropy of bond and structural stability. Elastic moduli for $BiGaO_3$ determined by perturbation method at equilibrium pressure within GGA and LDA approaches are listed in Table 2. It seems that our elastic constants are closer to other computation carried out within Wien2k computer code [29]. Elastic modulis computed by LDA are greater than those determined within GGA. Computed elastic moduli for $BiGaO_3$ are positive and satisfying the following generalized conditions to ensure their elastic stability [31]:

$$C_{11}+2C_{12}\rangle 0, C_{44}\rangle 0, C_{11}-C_{12}\rangle 0, C_{12}\langle B\langle C_{11} \quad (1)$$

It is noted that our calculated B value from elastic constants is closer to that given by fit Murnaghan. This proves that our calculated elastic constants are correct. The effect of pressure on elastic moduli is visualized in Fig. 2. We noticed that this compound show high elastic moduli. The elastic moduli of $BiGaO_3$ increase monotonously with increasing pressure, furthermore the variation on C_{44} is little sensitive to the pressure.

The computed elastic constants could be used to determine some physical and mechanical parameters as listed in Table 3. These parameters have been determined using Voigt [32], Reuss [33] and Hill [34] approximations. The Poisson's ratio of $BiGaO_3$ is closer to the limit value 0.25, so the bonding between Bi-6p and O-2p states is ionic [35]. The computed anisotropy factor value indicates that $BiGaO_3$ is isotropic. The greater B_H/G_H ratio values than 1.75 traduce the ductility of $BiGaO_3$. Bulk modulus is the resistance when volume changes under applied pressure. Shear modulus is the ratio of stress to strain. Young's modulus also called elasticity is the ratio of uniaxial stress to strain. Poisson's ratio is used to determine the bonding nature. The anisotropic elastic factor gives information about material properties in specific direction. We visualize these parameters in 3D dimensions using ELATE software [36]. We present in Fig. 3 the directional dependent of shear modulus, Young's modulus, linear compressibility and Poisson's ratio for $BiGaO_3$. Minimum and maximum of each parameter are visualized by green and blue colors. For isotropic material, the shape is spherical and any distortion from the spherical shape indicates anisotropy. From Fig. 3, we note that linear compressibility and Young's modulus are practically isotropic, while Poisson's ratio is anisotropic and little anisotropy is observed in shear modulus of $BiGaO_3$. The predicted maximum and minimum values of directional dependent of these parameters for $BiGaO_3$ are listed in Table 4.

3. 3. Debye temperature

The Debye temperature is an important fundamental parameter closely related to many physical properties such as specific heat and melting temperature. At low temperature, the vibrational excitations arise solely from acoustic vibrations. Hence, at low temperature, Debye temperature calculated from elastic constants is the same as that determined from specific heat measurements [3]. The standard method to calculate Debye temperature and longitudinal and shear waves velocity from elastic constants is found in references [37-39]. The computed Debye temperature for $BiGaO_3$ compound is reported in Table 2. Debye temperature computed with LDA is greater than that calculated by GGA. Predicted elastic wave velocities along [100], [110], [111] and [001] directions using GGA for $BiGaO_3$ are listed in Table 5. The GGA and LDA llongitudinal (shear) waves are fastest (slowest) along [111] direction for $BiGaO_3$.

3. 4. Electronic properties

We show in Fig. 4 electronic band structures along high symmetry Γ, R, M and X points for $BiGaO_3$ at equilibrium lattice constant. The band gap in $BiGaO_3$ is indirect type (M-X) with a value 1.254 eV. This value agrees reasonably with that 1.88 eV in $BiGaO_3$ calculated with GGA-PBE using Vienna ab initio Simulation Package [8]. The valence band is grouped into three distinct

regions with energy range -20 to E_F. The first two strips in the valence band region are located at (-8.25 eV to E_F) and (-12.75 to -9.08 eV). The first conduction band is situated at (E_F to 5.45 eV). We plot in Fig. 5 the dependence on pressure of direct and indirect band gaps between various symmetry points. One can notice that all energy gaps increase monotonously with increasing pressure in $BiGaO_3$. We display in Fig. 6 the dependence on pressure of the E_{M-X} and E_{R-X} indirect energy gap, which increases monotonously with increasing pressure in $BiGaO_3$ and changes from indirect E_{M-X} to indirect E_{R-X} at about 25 GPa. Total and partial densities of states in $BiGaO_3$ as shown in Fig. 7 reveal that the upper valence band is consisted principally of O-2p sites and a little contribution of Ga-4p and Bi-6p states. A part of first conduction band located between E_F and 2.39 eV is empty. Then transition occurs between O-2p and Bi-6p or Ga-4p. In the upper valence band, hybridization between Ga-4p orbital with O-2p site close to the Fermi level imply that Ga–O bonds have a covalent bonding character. There is also small contribution from 6p state of Bi in valence bands. However, Bi-6p state are dominating at the conduction band minima in confirmation with Bi atom's ionic bonding nature with O atom.

3. 5. Optical properties

The main optical spectrum due to the transition from five upper valence bands to five lower conduction bands requires knowledge of imaginary part of dielectric function. We display imaginary part versus photons energy in Fig. 8. Transition energy $E(k) = E_{cj}(k) - E_{vi}(k)$ is plotted in Fig. 9; where v_i and c_j are the valence band number i and the conduction band number j respectively. Threshold energy of dielectric function occurs at 1.65 eV, which corresponds to the fundamental indirect gap for $BiGaO_3$. We study transitions from occupied orbital O-2p to unoccupied site Bi-6p or Ga-4p. **F**irst peak positioned at 3.55 eV corresponds probably to transitions V_1–C_2 at M point, (V_1–C_1, V_2–C_1 or V_3–C_1) at R point or V_5–C_1 at X point. The second structure centered at 4.82 eV originates mainly from transitions V_1–C_1, V_2–C_1, V_4–C_1, V_1–C_2, V_5–C_2, V_4–C_2, V_5–C_1 at Γ point. For energy 6.82 eV, $BiGaO_3$ exhibit V_5–C_3, V_5–C_4 at X point and V_5–C_5, V_4–C_5, V_3–C_5, V_4–C_4, V_5–C_4, and V_3–C_3 transitions located near Γ point. Transitions V_2–C_5, V_4–C_5, V_5–C_5, can be observed at R point for energy 8.96 eV. Energy 11.85 eV is origin of V_5–C_5 transition positioned between M and R points. We plot the loss function spectra versus wavelength for $BiGaO_3$ in Fig. 10. We distinguish two regions for electronic loss function such as high loss function region located between 36.55 to 51 nm. The second region corresponds to wavelength less than 36.55 nm and greater than 51 nm. The first region is high loss region with change of wavelength after the ionization edge. The other is the lower loss function, which can provide information about composition and electronic structure. The loss function reaches

maximum value 8.81 at 42.3 nm for $BiGaO_3$. The amount of light that is incident on the surface of the photo catalytic material that can be estimated from the reflectivity, which is related to the absorbance of that material. We observe that reflectivity of $BiGaO_3$ as shown in Fig. 11 has a value 0.019, which corresponds to wavelength 31.9 nm. After successive aggrandizement, it reaches a maximum value 0.64 at 43 nm. It is reported, that lower reflectivity indicates higher UV light absorption [40]. **P**olycrystalline polarization method is used in calculation of optical absorption. During simulation, small smearing value 0.1 was applied to obtain more distinguishable absorbance peaks. The obtained absorption peaks as depicted in Fig. 12 are attributed to the photo transition energies from maximum valence band to minimum conduction band under UV light irradiation. The high value of absorption is 453302 cm^{-1} at wavelength of 44.8 nm. The high absorption value provides a hint that this material is a potential candidate as a photo catalyst in the degradation of chemicals or pollutants. It is noticed that maximum absorption corresponds to maximum reflectivity and no loss function.

3. 6. Thermodynamic properties

We study thermodynamic parameters of $BiGaO_3$ under temperature and pressure effect by applying quasi-harmonic Debye model. We carried out total energy versus unit cell volume. Thermal parameters are determined in temperature and pressure ranging from 0 to 1800 K and 0−50 GPa. We note that Debye model indicates that heat capacity is proportional to T^3 at low temperature and follows Dulong-Petit law at high temperatures. Fig. 13 presents volume – temperature diagram for $BiGaO_3$ at several pressures. The volume increases (decreases) when temperature (pressure) is enhanced. At 300 K and zero pressure, the lattice constant is 3.6728 Å. Fig. 14 shows the temperature effect on bulk modulus. The compressibility decreases (increases) with increasing temperature (pressure). At 300 K and zero pressure, compressibility is equal to 170.13 GPa. Fig. 15 displays the effect of temperature and pressure Debye temperature. Debye temperature is practically constant between 0 and 300 K, and then follows a linear decrease. It is noted that Debye temperature is enhanced under pressure effect. At 300 K and zero pressure, θ_D is 457.34 K, which is closer to that estimated by elastic constants with GGA. We plot in Fig. 16 the variation of the volumetric thermal expansion coefficients α versus temperature. It is shown that α increases sharply up to 500 K, then it follows a linear increase. At T=300 K, P=0 GPa, α is 2.93×10^5 K^{-1}. At high temperature, the constant volume heat capacity tends to the Dulong–Petit limit [41], while at low temperature, it is proportional to T^3 [42]. Figs. 17 and 18 represent the variation of the constant volume and pressure heat capacities versus temperature. From 0 to 500 K, C_V and C_P increase exponentially and the difference between them is very slight. At high temperature (T > 500 K) C_P

follows a linear increase whereas C_V tends to Dulong - Petit limit. At high temperature C_V tends to approach $122.79\ Jmol^{-1}K^{-1}$. At zero pressure and ambient temperature, the C_V and C_P are $111.34\ Jmol^{-1}K^{-1}$ and 111.34 $mol^{-1}K^{-1}$, respectively. Fig. 19 represents the dependence on temperature and pressure of theoretical entropy S. The shape of the curve is exponential. At zero pressure and 300 K, the entropy is 120.66 $J.mol^{-1}K^{-1}$ for ScF_3. The predicted constant pressure and volume heat capacities and entropy using GGA for $BiGaO_3$ are listed in Table 6.

4. Conclusion

$BiGaO_3$ was studied by PP-PW method of DFT within GGA and LDA. Equilibrium lattice constant and bulk modulus are closer to theoretical one. Elastic moduli follow a linear dependence on pressure. Shear and Young's moduli, Poisson's ratio, average sound velocities and Debye temperature are estimated in the frame work of Voigt-Reuss-Hill approximations for $BiGaO_3$ polycrystalline aggregates. The higher absorption value of $BiGaO_3$ provides that this material is a potential candidate as a photo catalyst in the degradation of chemicals or pollutants. Bi-6p state is dominating at the conduction band minima in confirmation with Bi atom's ionic bonding nature with O one. Threshold energy of dielectric function corresponds to the fundamental indirect band gap for $BiGaO_3$. We predicted constants pressure and volume heat capacities and entropy using GGA for $BiGaO_3$.

Acknowledgment

The authors acknowledge Taif University Research Supporting Project number (TURSP-2020/66), Taif University, Taif, Saudi Arabia.

References

[1] S. W. Cheong, M. Mostovoy, Nat. Mater. 6 (2007) 13.

[2] A. A. Belik, J. Solid State Chem. 195 (2012) 32.

[3] P. Baettig, Ch.F. Schelle, R. Lesar, U.V. Waghmare, N.A. Spaldin, Chem. Mater. 17 (2005) 1376.

[4] N.A. Hill, K.M. Rabe, Phys. Rev. B 59 (1999) 8759.

[5] R. Seshadri, N.A. Hill, Chem. Mater. 13 (2001) 2892.

[6] J. Kaczkowski, A. Jezierski, Acta. Phys. Pol. A 124 (2013) 852.

[7] A. Kourdassi, N. Benkhettou, M. Labair, M. Benkabou, S. Benalia, R. Khenata, H. Baltache, Djamel Rached, Braz. J. Phys. 44 (2014) 914.

[8] J. Kaczkowski, J. Alloy. Compd. 613 (2014) 175.

[9] C. Li, B. Wang, R. Wang, H. Wang, X. Lu, Comp. Mater. Sci. 42 (2008) 614.

[10] C. Li, Z. Wang, D. Ma, C. Wang, B. Wang, J. Phys. D: Appl. Phys. 47 (2014) 055302.

[11] A.A. Belik, T. Wuernisha, T. Kamiyama, et al., Chem. Mater. 18 (2006) 133.

[12] A.A. Belik, J. Solid State Chem. 195 (2012) 32.

[13] J.Z. Zhang, H.C. Ding, J.J. Zhu, Y.W. Li, Z.G. Hu, C.G. Duan, X.J. Meng, J.H. Chu, J. Appl. Phys. 115 (2014) 083110.

[14] A.A. Belik, S.Y. Stefanovich, B.I. Lazoryak, E. Takayama-Muromachi, Chem. Mater. 18 (2006) 1964.

[15] M.D. Segall, P.J.D. Lindan, M.J. Probert, C.J. Pickard, P.J. Hasnip, S.J. Clark, M.C. Payne, J. Phys.: Condens. Matter 14 (2002) 2717.

[16] P. Hohenberg, W. Kohn, Phys. Rev. B 136 (1964) 864.

[17] W. Kohn, L.J. Sham, Phys. Rev. A 140 (1965) 1133.

[18] D. Vanderbilt, Phys. Rev. B 41 (1990) 7892.

[19] J.P. Perdew, K. Burke, M. Ernzerhof, Phys. Rev. Lett. 77 (1996) 3865.

[20] S. Goedecker, M. Teter, and J. Hutter, Phys. Rev. B 54 1703 (1996).

[21] H.J. Monkhorst, J.D. Pack, Phys. Rev. B 13 (1976) 5188.

[22] T.H. Fischer, J. Almlof, J. Phys. Chem. 96 (1992) 9768.

[23] M. A. Blanco, E. Francisco, V. Luaña, Comput. Phys. Commun. 158 (2004) 57.

[24] M. A. Blanco, A. M. Pendás, E. Francisco, J. M. Recio, R. Franco, J. Molec. Struct. Theochem. 368 (1996) 245.

[25] M. Flórez, J. M. Recio, E. Francisco, M. A. Blanco, A. M. Pendás, Phys. Rev. B 66 (2002) 144112.

[26] E. Francisco, J. M. Recio, M. A. Blanco, A. M. Pendás, J. Phys. Chem. 102 (1998) 1595.

[27] E. Francisco, M. A. Blanco, G. Sanjurjo, Phys. Rev. B 63 (2001) 049107.

[28] F.D. Murnaghan, Proc. Nat1. Acad. Sci. USA 30 (1994) 244.

[29] Rasul Bakhsh Behram, M.A. Iqbal, S.M. Alay-e-Abbas, M. Sajjad, M. Yaseen, M. Imran Arshad, G. Murtaza, Materials Sciencein Semiconductor Processing 41 (2016) 297–303.

[30] J.M. Legér, B. Blanzat, J. Mater. Sci. Lett. 13 (1994) 1688.

[31] W. Voigt, Lehrbuch der Kristallphysik (Teubner, Leipzig, 1928).

[32] W. Voigt, Lehrbuch der Kristallphysik (Teubner, Leipzig, 1928).

[33] A. Reuss, Z. Angew, Math. Mech. 9 (1929) 49-58.

[34] R. Hill, Proc. Phys. Soc. London A 65 (1952) 349.

[35] Gencer A, Surucu G. Electronic and lattice dynamical properties of Ti_2SiB MAX phase. Mater Res Express 2018;5:076303.

[36] M. Mattesini, M. Magnuson, F. Tasnádi, C. Höglund, Igor A. Abrikosov, L. Hultman, Phys. Rev. B 79 (2009) 125122.

[37] O.L. Anderson, J. Phys. Chem. Solids 24 (1963) 909.

[38] E. Schreiber, O.L. Anderson, N. Soga, Elastic Constants and Their Measurements, McGraw-Hill (New York), (1973).

[39] B. B. Karki, L. Stixrude, S. J. Clark, M. C. Warren, G. J. Ackland, J. Crain, Am. Mineral 82 (1977) 51.

[40] Berning PHH, G;Madden, R. P. 1960. JOSA 50: 586-97.

[41] A.T. Petit, P.L. Dulong, Ann. Chim. Phys. 10 (1819) 395.

[42] P. Debye, Ann. Phys. 39 (1912) 789.

Figures

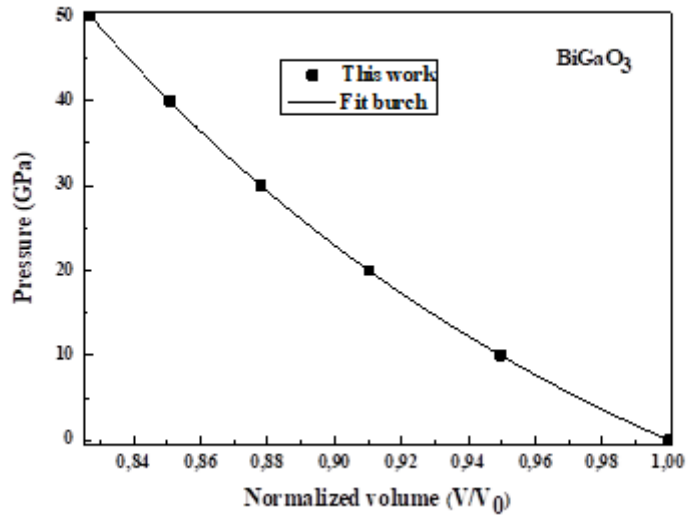

Figure 1

The pressure dependence on normalized volume for BiGaO3.

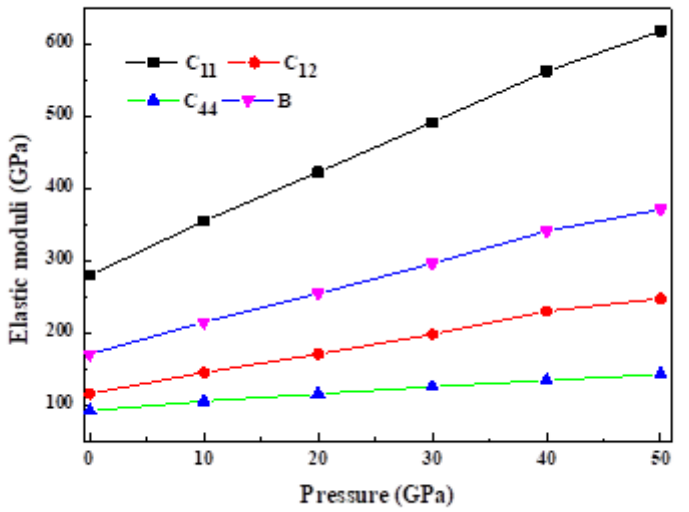

Figure 2

The plotted elastic moduli as a function of pressure for BiGaO3.

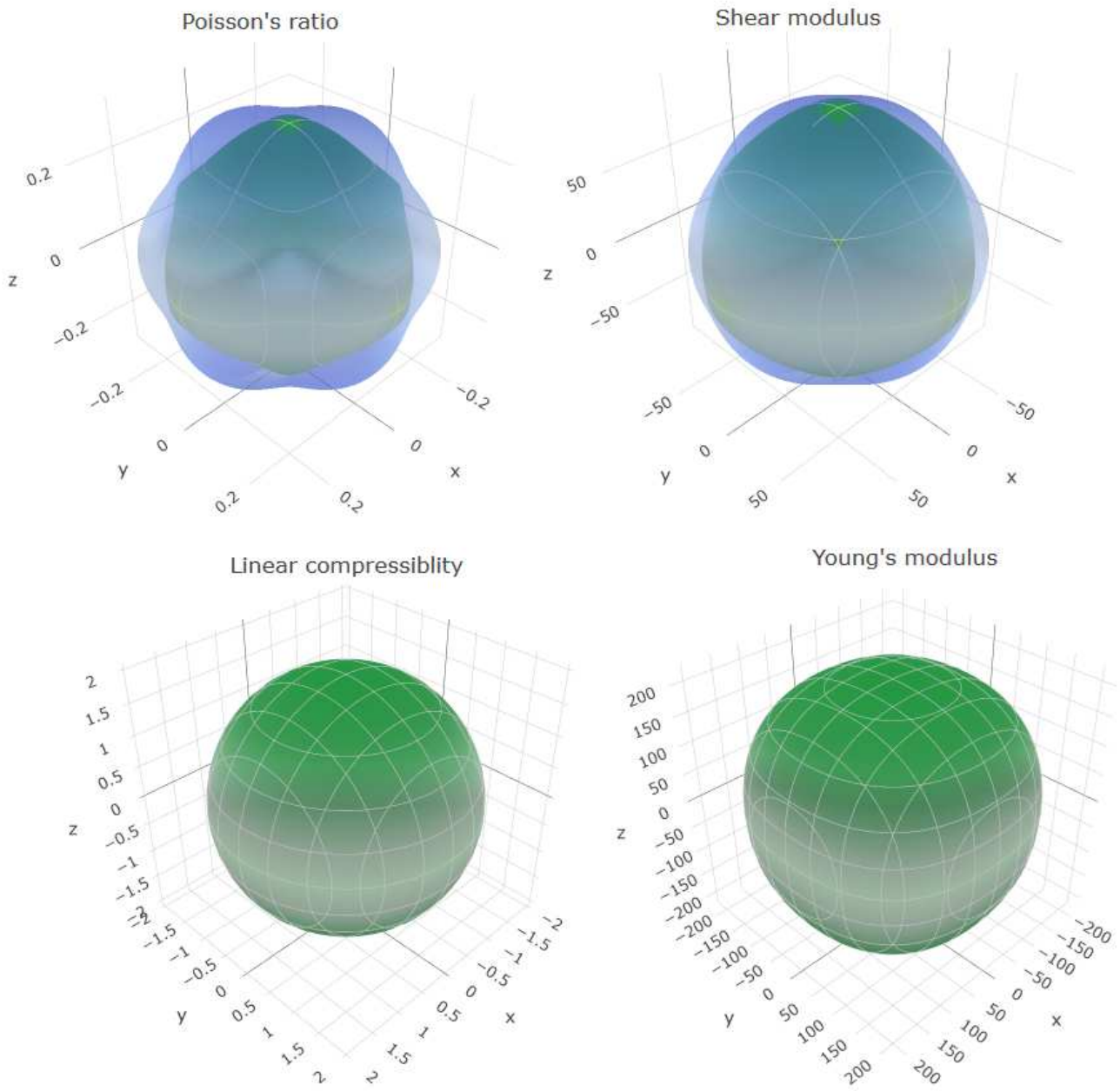

Figure 3

The directional dependent shear modulus, Young's modulus, linear compressibility and Poisson's ratio for BiGaO3.

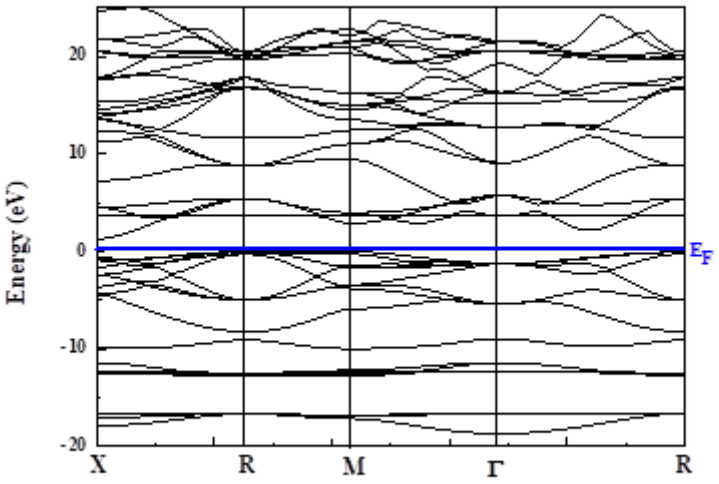

Figure 4

The band structure of BiGaO3 at various symetry points in the Brillouin zone.

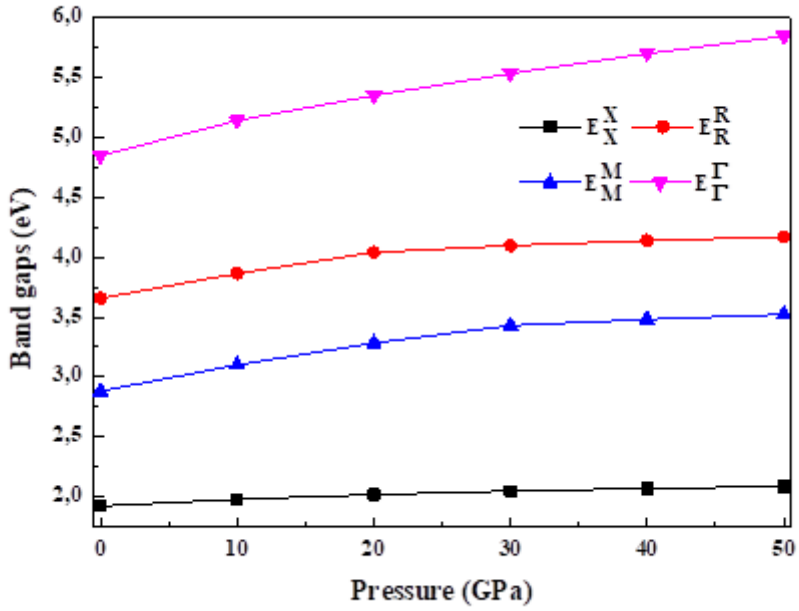

Figure 5

The dependence on pressure of direct and indirect gaps for BiGaO3.

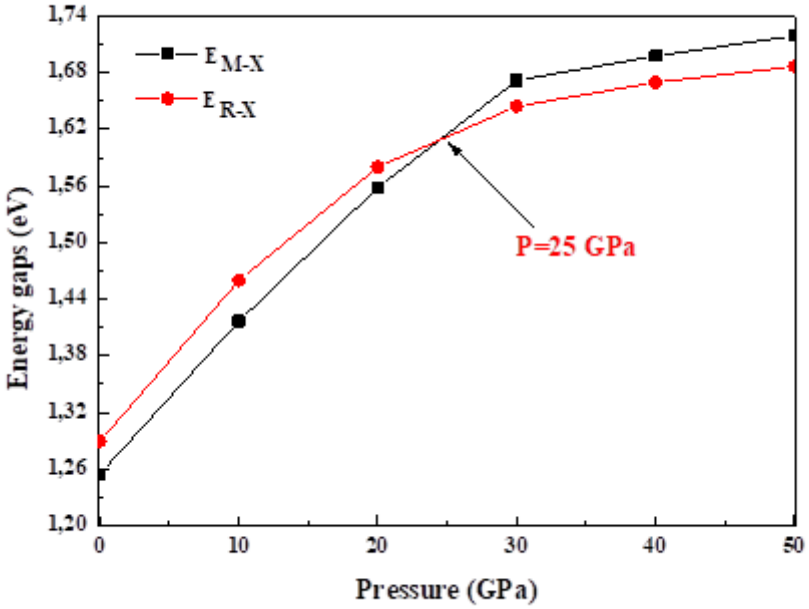

Figure 6

The fundamental gap as a function of pressure.

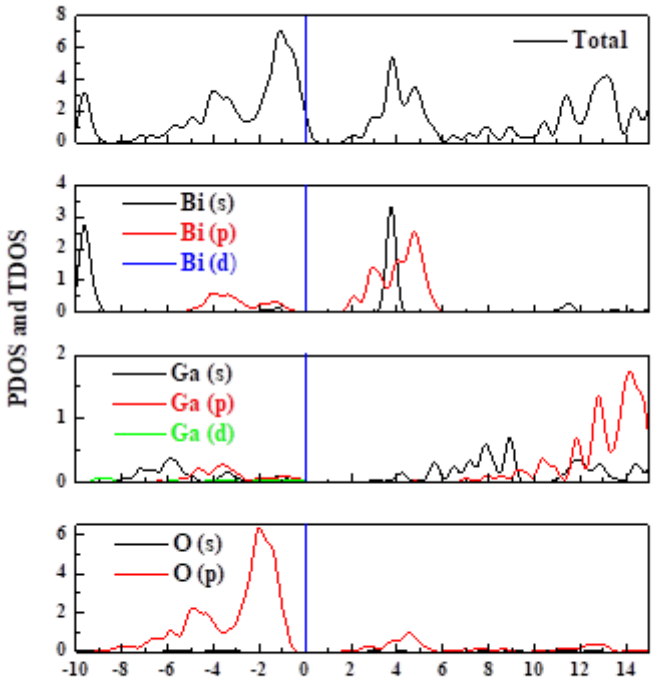

Figure 7

The total and partial densities of states (TDOS) and PDOS of of BiGaO3.

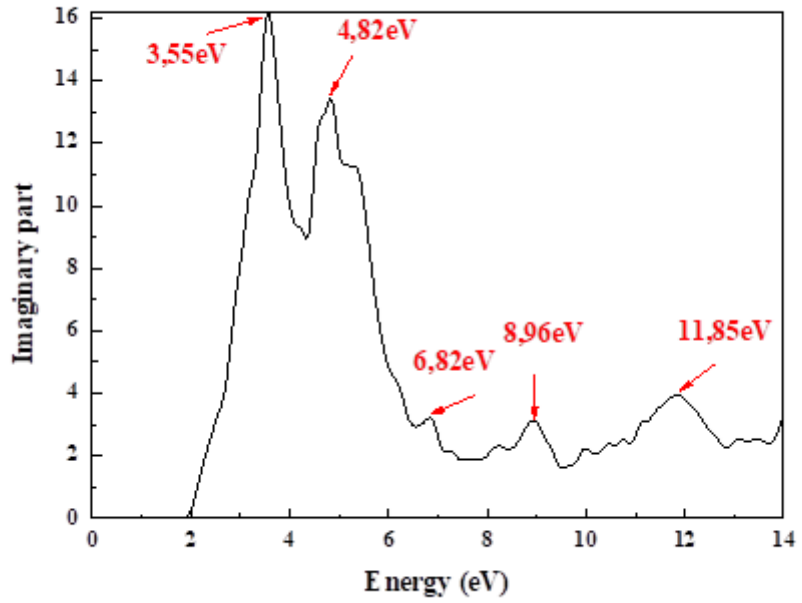

Figure 8

Imaginary part of the dielectric function versus photon energy.

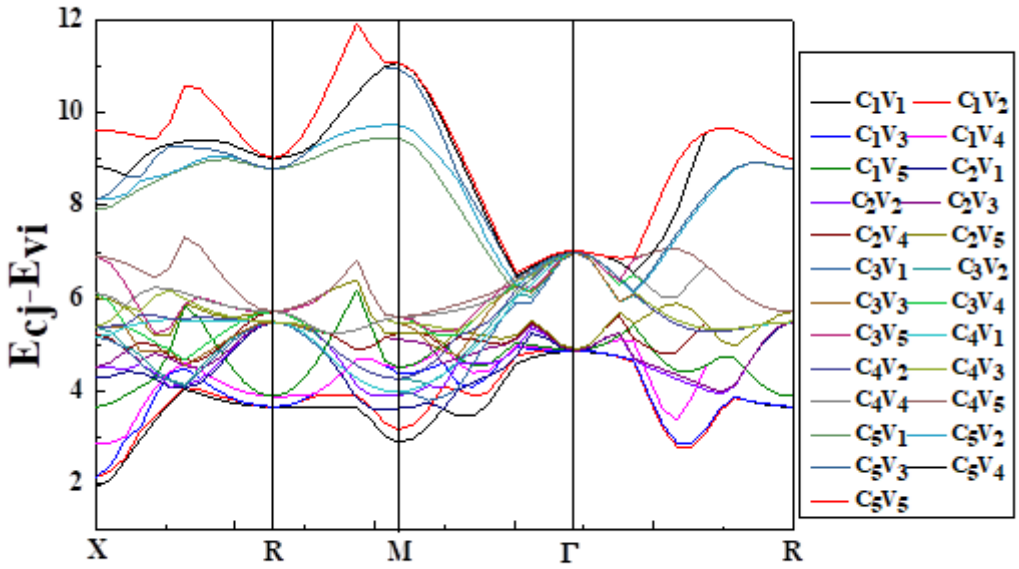

Figure 9

The transition energy E(k) = Ecj(k) – Evi(k).

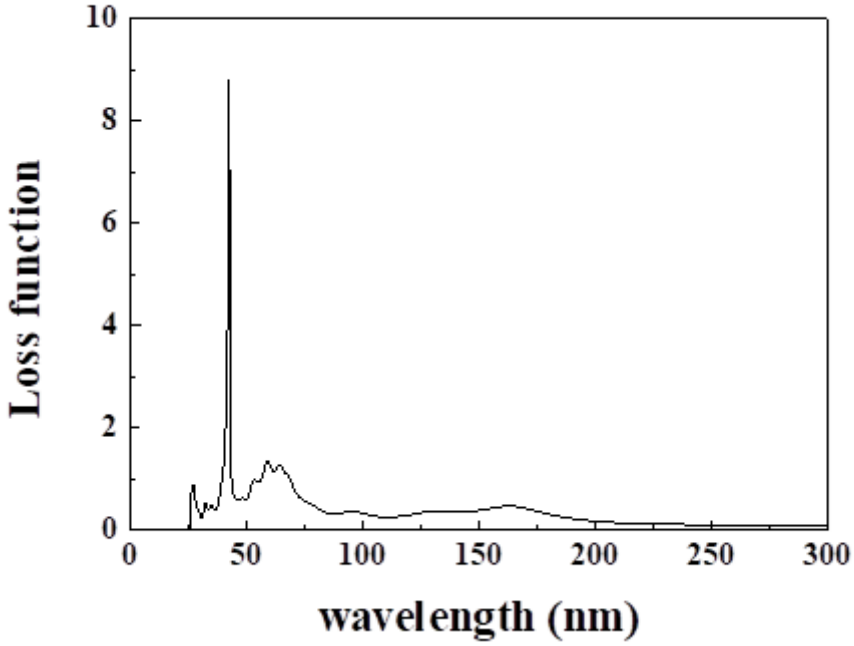

Figure 10

The loss function as a function of wavelength.

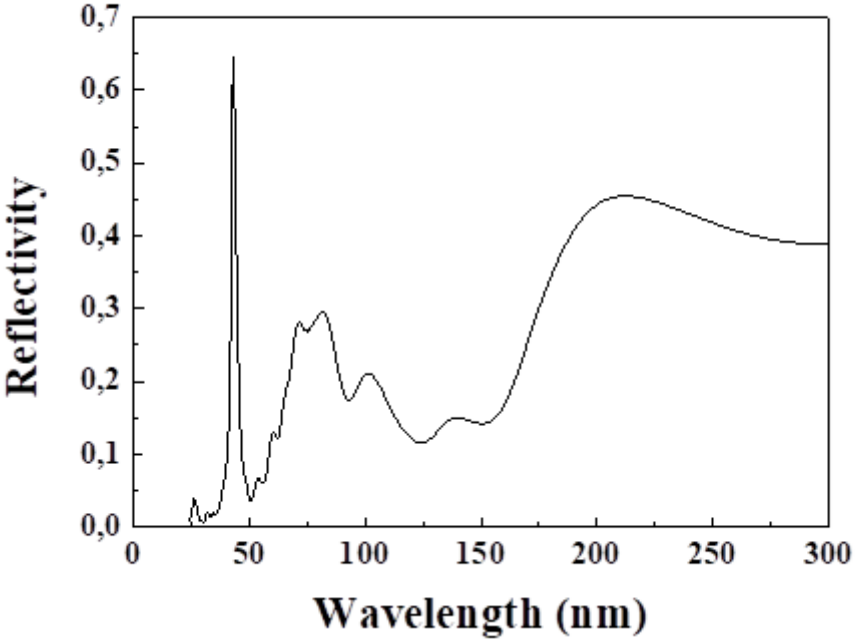

Figure 11

The reflectivity as a function of wavelength.

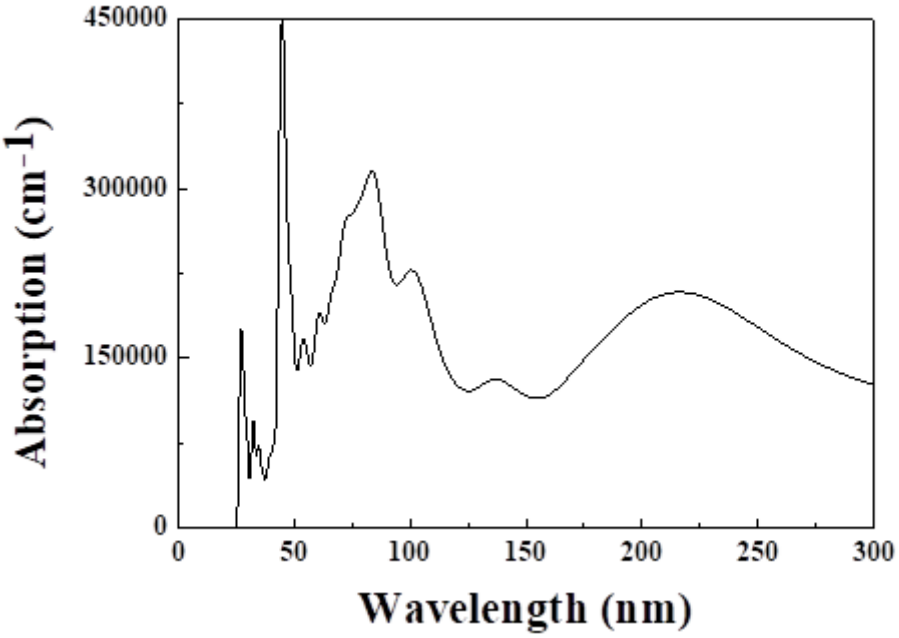

Figure 12

The absorption as a function of wavelength.

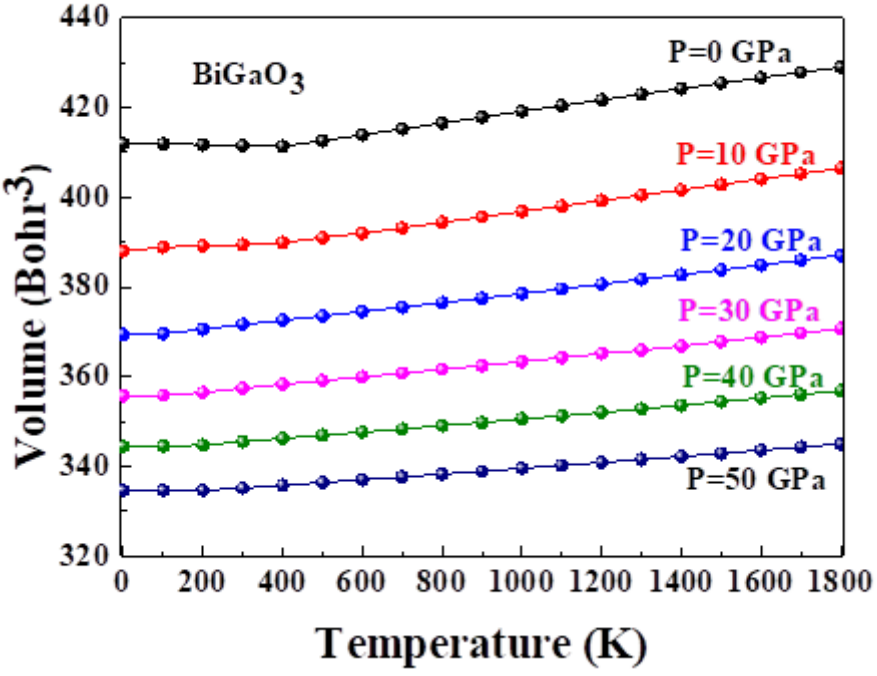

Figure 13

The volume_temperature diagram of BiGaO3.

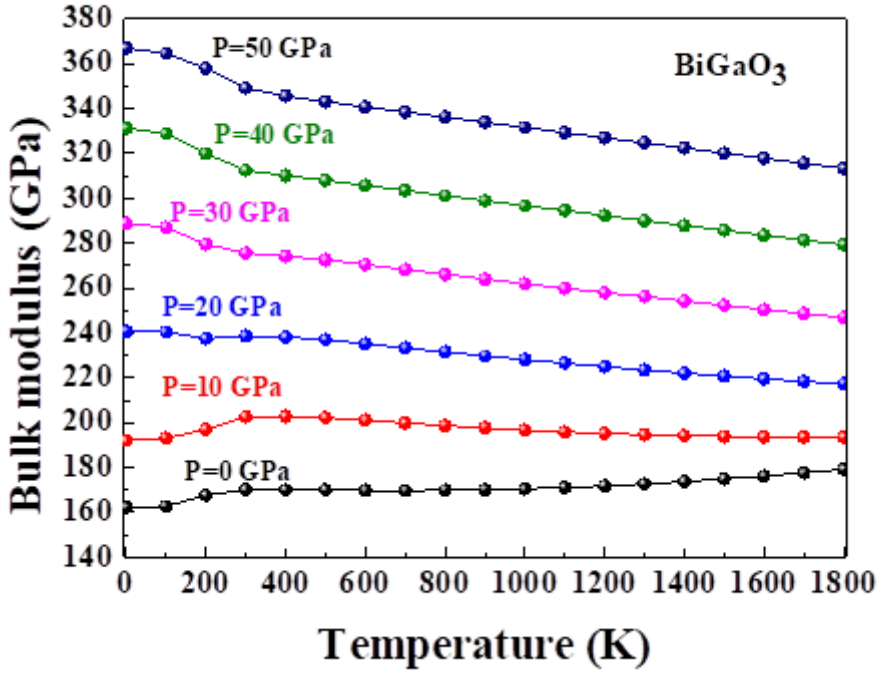

Figure 14

The bulk modulus as a function of temperature for BiGaO3.

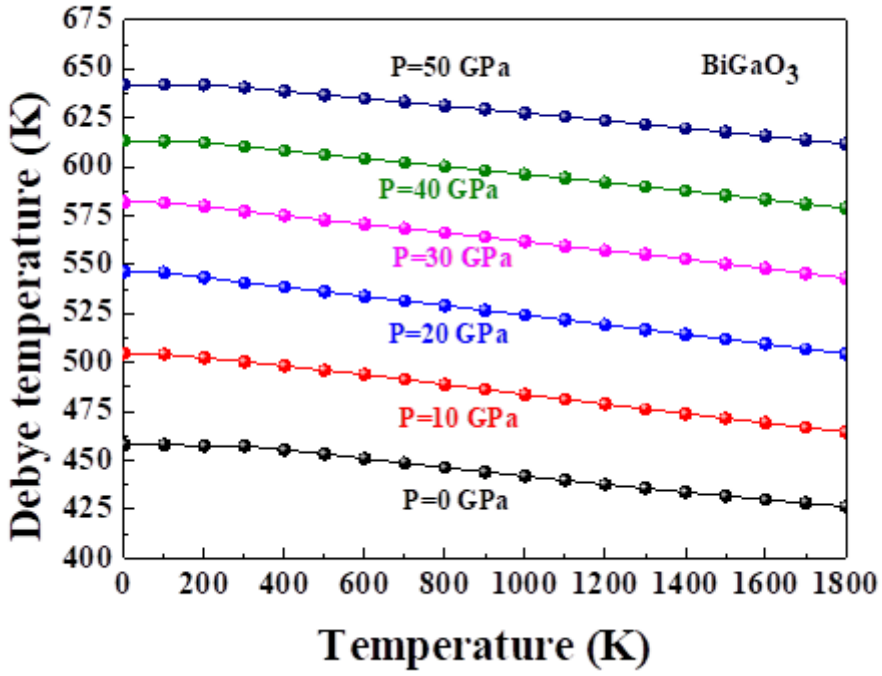

Figure 15

The dependence of Debye temperature on temperature for BiGaO3.

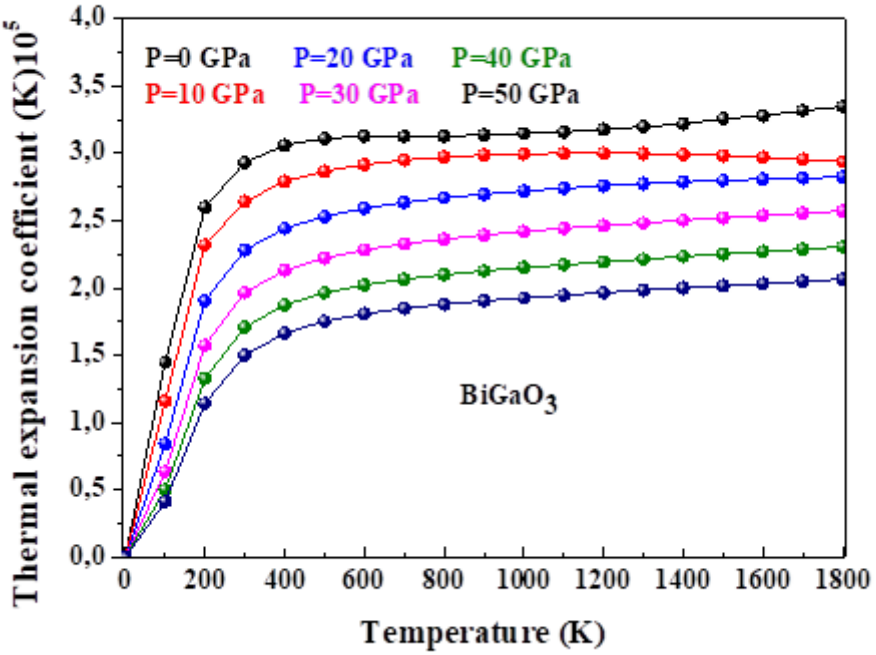

Figure 16

The volumetric thermal expansion coefficients as a function of temperature

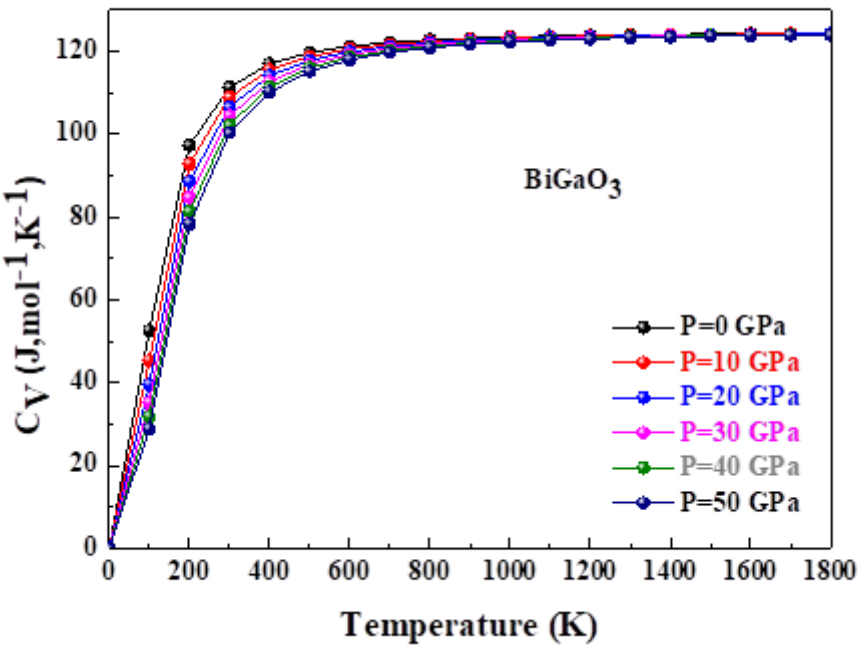

Figure 17

The constant volume heat capacity as function of temperature.

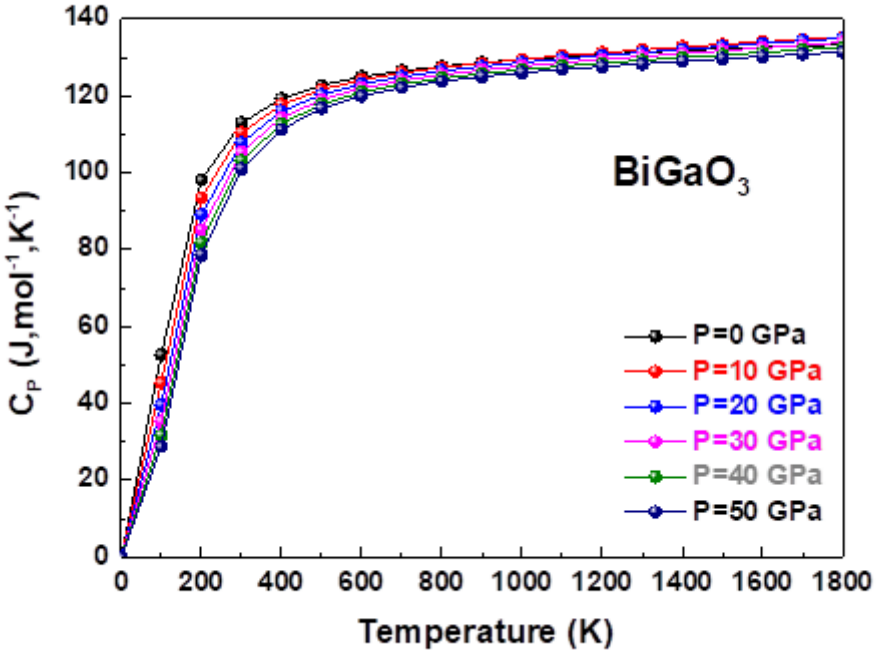

Figure 18

The constant volume heat capacity as function of temperature.

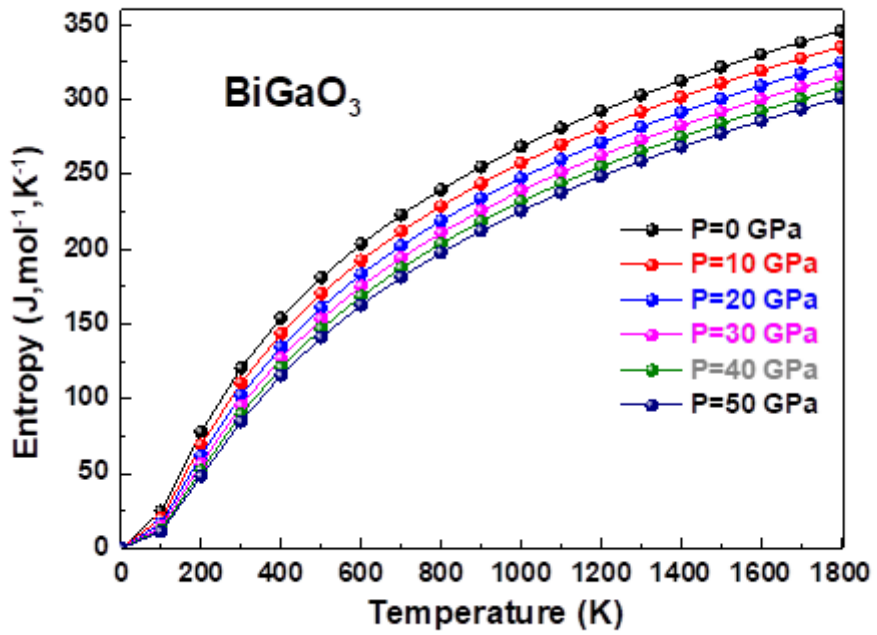

Figure 19

The dependence of theoretical entropy S on temperature.